Acta Manilana 72 (2024), 68-80

ISSN: 0065-1370

Acta Manilana

journal homepage: https://actamanilana.ust.edu.ph/

Waste to Power: Optimization of Pyrolysis and Treatment Conditions of Rice Straw Biochar as Electrode Material for Supercapacitor Application

David Joseph G. Alzate[1], Felicidad Christina R. Peñafiel[2,3], and Christina A. Binag[1,2,3]*

[1]The Graduate School, University of Santo Tomas, España Blvd., 1015 Manila, Philippines
[2]Research Center for the Natural and Applied Sciences, University of Santo Tomas, España Blvd., 1015 Manila, Philippines
[3]Department of Chemistry, College of Science, University of Santo Tomas, España Blvd., 1015 Manila, Philippines

Graphical Abstract

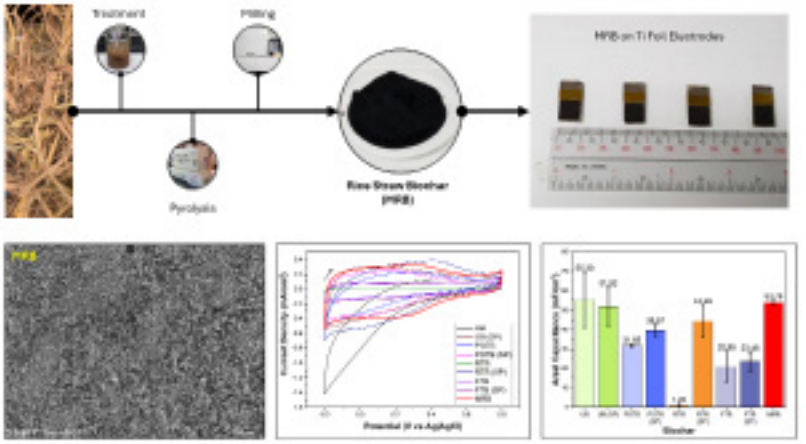

Abstract

Supercapacitors, known for high power and long cycle lives, can be made from sustainable materials like biochar, which is highly porous and derived from abundant raw materials. Rice straw is converted into biochar via pyrolysis in a tube furnace under N_2. Various treatments were explored to enhance biochar's porosity and capacitance: (1) varying pyrolysis temperatures (700, 800, 900 °C), (2) chemical treatments (HNO_3 treatment before and after pyrolysis, reflux with HNO_3, and high-temperature flash), and (3) physical treatments (carbon black spiking and wet-milling with a planetary ball mill). Biochar pyrolyzed at 700 °C showed higher areal capacitance values than those at higher temperatures. Untreated biochar (UB) had the highest capacitance (55.30 mF/cm² at 5 mV/s), followed by post-treated biochar (POTB) at 31.65 mF/cm². Carbon black spiking further improved these values. BET analysis revealed UB had a lower surface area and pore volume (44.10 m²/g and 0.0142 m³/g). HNO_3 treatment (167.66 m²/g and 0.0916 m³/g) and milling (224.85 m²/g and 0.2257 m³/g) significantly increased these metrics. Milled biochar (MRB) achieved 53.76 mF/cm² capacitance with better repeatability, highlighting that optimizing the preparation conditions of rice straw biochar can significantly increase its porosity, surface area, and electrochemical performance, repurposing the agricultural waste for supercapacitor applications.

Keywords: rice straw biochar; supercapacitor; EDLC

Corresponding authors: cabinag@ust.edu.ph
DOI: https://doi.org/10.53603/actamanil.72.2024.hawe3780

Date Received: 19 August 2024
Date Revised: 03 September 2024
Date Accepted: 06 November 2024

Introduction

Rice straw is a waste by-product from harvesting rice. In a 2020 study by Balingbing and colleagues, the Philippines produces 18 million tons of this agricultural waste per year, of which 95% usually burned [1]. This practice can further worsen air quality and have climate change complications. Repurposing rice straw as a composite material for energy storage electrodes offers a sustainable and desirable alternative. This approach transforms rice straw into a more useful resource and addresses energy availability and accessibility, particularly in remote and rural areas.

Supercapacitors are a type of energy storage device that is an intermediary between batteries and traditional capacitors. They offer rapid charge-discharge cycles along with substantial energy storage capacity [2]. The electrode is crucial for storing energy in supercapacitors; thus, improving the electrode best enhances the device's overall electrochemical performance [2,3]. Biochar and similar carbon materials are classified as electric double-layer capacitor (EDLC) materials. They store charge electrostatically on their surface using reversible adsorption of the electrolyte ions. Ideally, an ELDC electrode should have high porosity and surface area, good conductivity, and electrochemical stability. Biochar is a good candidate for an EDLC material because of its high porosity and surface area, and its surface characteristics may be further enhanced with the proper treatment and pyrolysis conditions. It is also low-cost, highly renewable, and widely available. This study explores the enhancement of rice straw biochar to improve its performance as a supercapacitor electrode.

Materials and methods

The chemicals and reagents are analytical grade unless otherwise stated. They were procured from a local supplier and used as instructed. Rice straw was procured from Nueva Ecija, Philippines, and sun-dried before any procedure. Water (DI H_2O) used to prepare solutions was deionized with a Millipore Elix Advantage 10 water purifier. Carbon black (Super P®) was obtained from Korea.

Treatments and pyrolysis of rice straw biomass to biochar. The preparation of biochar was adopted from the works of Genovese and colleagues [4], Jiang and colleagues [5], and Kim and colleagues [6]. Rice straw was pre-dried in the oven at 120 °C then finely crushed using a coffee grinder. The powder was sifted through ASTM Standard Test Sieves (850 um > 425 um). For control biochar, the biomass was pyrolyzed without pretreatment into a Daihan Tube Furnace at (700 °C, 800 °C, or 900 °C) for 1 h at a rate of 5 °C per min under N_2 atmosphere.

For modified biochar, the biomass was first pretreated in 1M HNO_3 (10 mL g^{-1}) at 75 °C for 4 h under constant stirring. The resulting pretreated biomass was rinsed repeatedly with DI H_2O to pH 7, dried, then pyrolyzed at (700 °C, 800 °C, or 900 °C) for 1 h at a rate of 5 °C per min under a nitrogen atmosphere. The biochar was post-treated in 5 M HNO_3 (20 mL g^{-1}) for 4 h under constant stirring. After this, the post-treated biochar was rinsed repeatedly with DI H_2O to pH 7 and dried.

The preparation of refluxed treated biochar was derived from the works of Gomez-Martin and colleagues [7] and Pourhosseini and colleagues [8]. Pre-treated biochar was refluxed in 5 M HNO_3 at 20 mL g^{-1} for 4 h. The resulting refluxed biochar was rinsed repeatedly with DI H_2O to pH 7 and dried.

For high-temperature flashed-treated biochar, its preparation was adopted from the works of Genovese and colleagues [4]. Pretreated biochar was post-treated in 5 M HNO_3 (20 mL g^{-1}) for 4 h under constant stirring. After this, the post-treated biochar was rinsed repeatedly with DI H_2O to pH 7 and dried. The biochar was placed in a ceramic crucible and then flashed pyrolyzed in a muffle furnace (Daihan) for 1 min at 950 °C.

For the wet-milling process of biochar, its preparation was derived from the works of Peterson and colleagues [9], Lyu and colleagues [10], and Lyu and colleagues [11]. Biochar and carbon black were combined in a zirconia milling pot at a 9:1 weight ratio. Zirconia milling balls (Ø = 5 mm; 100:1 zirconia balls:carbon, w/w) were added after, followed by DI H_2O to fully submerge the balls. The mixture was processed in a planetary ball mill (Jinan-Francis) at 300 rpm for 3 h clockwise, allowed to rest for 30 min, and then milled for another 3 h counter-clockwise. After milling, the zirconia balls were removed, the water was decanted, and the resulting carbon slurry was thoroughly dried in a vacuum oven at 70 °C.

Preparation of biochar slurry for Ti foil electrodes. This procedure was adapted from the works of Ding and colleagues [12] and Huang and colleagues [13]. Ten milligrams (10 mg) of polyvinylidene fluoride (PVDF) were dissolved in 800 µL dimethyl sulfoxide (DMSO). Prepared biochar was finely ground using an agate mortar and pestle. Ninety milligrams (90 mg) of the prepared biochar, or a mixture of 80 mg biochar and 10 mg carbon black, were added to the PVDF/DMSO solution. The slurries were stirred for at least 6 h or overnight.

Preparation of Ti foil electrodes. Pure titanium foil (0.15 mm thickness, Nilaco) was cut into 1 cm x 2 cm portions. Kapton tape was used over one side of the Ti foil and isolated a 1 cm x 1 cm active area on the other side. The active area was scuffed with 1000-grit sandpaper before each use. After scuffing, the Ti plate was placed in DI H_2O, sonicated for 15 min, then dried. Ten microliters (10 µL) of the biochar slurry were drop cast onto the active area of the foil and then spread carefully for full coverage. The biochar/Ti foils were dried in the oven at 70 °C for 2 h. This was used as the working electrode of the three-electrode setup.

Physical characterizations. The SEM micrographs of the composites were taken with a Hitachi SU3800 Variable Pressure Floor Type Scanning Electron Microscope. The samples were analyzed at 5 kV accelerating voltage.

The FTIR spectra of the composites was taken with a Shimadzu IR Prestige-21 with Diffuse Reflectance Spectroscopic (DRS-8000) attachment. The samples were ground with dry KBr (AR) and then scanned from 400 cm^{-1} to 4000 cm^{-1}.

The surface area and pore volume of the biochar samples were measured using a NovaTouch LX2 (Quantachrome Instruments). Samples were degassed under vacuum at 300 °C for 8 hours before analysis. Surface area was determined from adsorption data using the Brunauer-Emmett-Teller (BET) method at 0.01 – 0.3 relative pressure range, while pore volumes were calculated from desorption isotherm leg data using Barrett-Joyner-Halenda (BJH) theory.

Electrochemical characterizations. Cyclic voltammetry studies were conducted using a Biologic VSP-300 potentiostat, with the biochar/Ti foil electrodes as the working electrode, Ag|AgCl was used as the reference electrode, and a Pt coil was used as the counter electrode. One molar H_2SO_4 was used as the electrolyte and the potential window was set to -0.20 V to 0.80 V, and a scan rate of 5 mV/s

Results and Discussion

Several treatment methods were done on rice straw biochar to improve and enhance its porosity and electrochemical performance. Pyrolysis temperature changes, chemical and physical treatments were analyzed and optimized. Pyrolysis temperatures affect the degree of carbonization, surface groups, and porosity of the biochar [4,14,15]. Chemical activation of biomass is reported in the literature to enhance the surface and pore properties of the material [4,6,16], while post-pyrolysis chemical activation added surface functionalities onto the biochar's surface [4,5,7,8]. Alternatively, introducing a highly conductive carbon material such as carbon black at low quantities can help improve the electrochemical properties of the biochar [17]. Wet milling with a planetary ball mill was used to finely grind the biochar and improve the surface area and its characteristics. A higher surface area, as well as smaller pore diameters (Ø < 2 nm), should presumably lead to better electroactivity of the electrode composites [16].

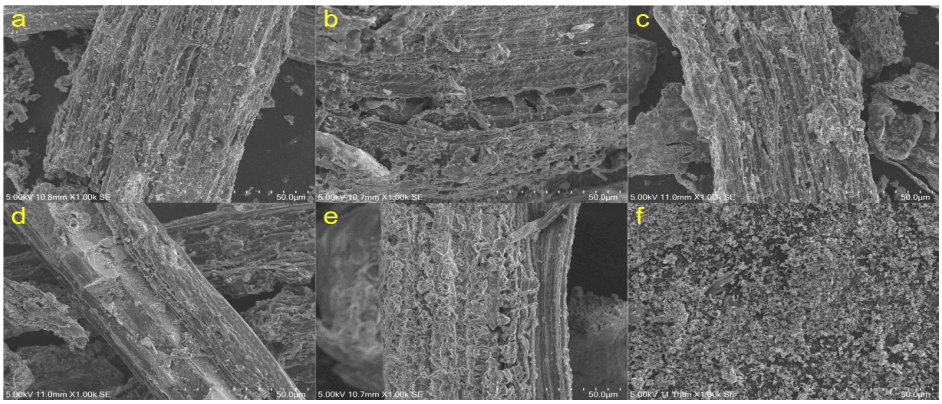

Figure 1. SEM micrographs of (a) unmodified biochar (UB), (b) pretreated biochar (PRTB), (c) post-treated biochar (POTB), (d) high-temperature flash-treated biochar (FTB), (e) reflux-treated biochar (RTB), and (f) milled biochar (MRB) at 1000x magnification.

Table 1. FTIR peaks observed for rice straw and its pyrolysis into biochar.

Wavenumber, cm^{-1}	Functional Group
3400	Alcoholic or phenolic -OH
3200	Aliphatic -CH
1740	Carbonyl C=O
1600	Aromatic C=C or conjugated C=O
1500	Cellulose transformation products, -CH and C=C
1450	Aromatic C=C
1360	Alkene C-H deformation
1100	C-O-C ether, pyranose ring
900 - 865	Aromatic C-H

SEM analysis. The micrographs of the biochar (Figure 1 (a – c)) show that the varied structures of the rice straw were preserved, such as the honeycomb and capillary structures. This is beneficial for the resulting biochar, as these structures serve as macropores (Ø > 2 μm), which provide additional sites for electrochemical activity, further formation of micropores, and lead to an overall higher surface area of the material [14,17]. Smaller pores (Ø < 2 μm) were also observed, these form from the cell structure's degradation during pyrolysis, leaving only the carbonaceous skeleton [14], and from HNO_3 treatment of the sample [4–6,17]. Similar structures were found in the RTB and FTB samples (Figure 1 (d) and (e)). After the wet milling process, Figure 1(f) shows the greatly reduced the particle size of the biochar MRB. BET analysis was employed to get a quantified increase in the porosity and surface area of the biochar.

Effect of pyrolysis temperature. Rice straw is composed primarily of 37.60 – 46.55 % cellulose, 22.35 – 28.25 % hemicellulose, and 5.60 – 11.60 % lignin [18,19], with their functional groups reflected in the IR spectra (Figure 2(a)), while Table 1 lists these major functional groups. The 3400 cm^{-1} and 3200 cm^{-1} peaks indicate alcoholic or phenolic -OH and aliphatic -CH groups, respectively. The peak around 1740 cm^{-1} corresponds to carbonyl -C=O groups. The peak near 1600 cm^{-1} is associated with aromatic C=C or conjugated C=O groups, while the peak around 1500 cm^{-1} pertains to C=C and -CH groups. Peaks at 1450 cm^{-1} and 1360 cm^{-1} correspond to aromatic C=C and alkene C-H deformation, respectively. Finally, the peaks around 1100 cm^{-1} and 900 - 865 cm^{-1} are characteristic of C-O-C ether and pyranose ring groups and aromatic -CH, respectively [6,18].

After pyrolyzing crushed rice straw to untreated biochar (UB), the intensity of -OH and -CH groups decreased with rising temperatures due to the dehydration and depolymerization of cellulose and hemicellulose [20] as seen in Figure 2(b). In contrast, the peaks around 900–865 cm^{-1} and 1450 cm^{-1} indicated significant dehydration and the increased formation of polycyclic aromatic structures, intensifying at higher temperatures [14,20], as seen in Figures 2(b – d). Similarly, peaks at 1360 cm^{-1} and 1500 cm^{-1}, linked to the decomposition and condensation of cellulosic and lignin components, showed a slight increase in intensity, suggesting the formation of graphitic structures, although this also results in the loss of most non-carbon atoms [20]. However, the C-O-C peak at 1100 cm^{-1} showed only a slight reduction, indicating the retention of the ether/pyranose ring structure [6,14,20].

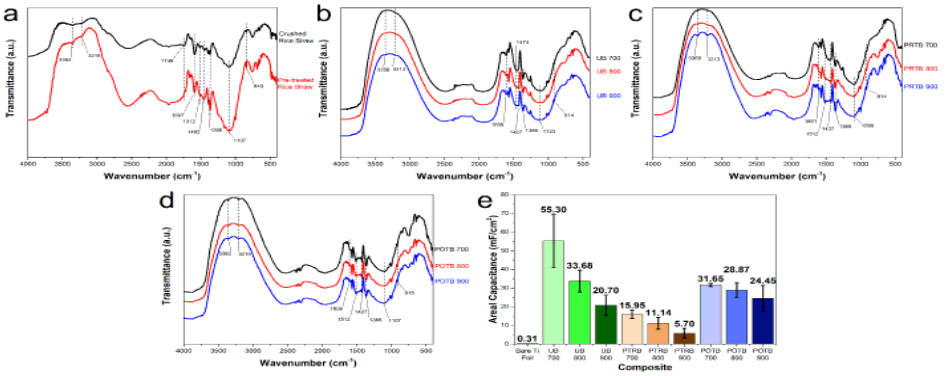

Figure 2. The FTIR spectra of (a) crushed rice straw and treated rice straw; (b) UB, (c) PRTB, and (d) POTB at increasing pyrolysis temperatures; and (e) bar graph of the areal capacitances of the composites derived from cyclic voltammetry.

When comparing the capacitances of the electrodes, the biochar samples showed a decreasing trend as the pyrolysis temperature increased as shown in Figure 2(e) and Table 2. This is likely due to higher carbonization and the loss of -O_x and -N_x groups at increasing temperatures [4,14]. Although high carbon content and surface area typically enhance conductivity and capacitance [15,16], the disordered graphitic structure and large macroparticle size of biochar can hinder electronic and ionic conductivity [4]. Many surface functional groups that promote pseudocapacitive reactions, such as hydroxyl, quinone, and pyrone structures, are either burned off at high temperatures [4,5,16], or decompose to low capacitance carboxyl and ester groups [4,6], further explaining the decreasing capacitance trend. This shows that the capacitance of biochar is not solely attributed to conductivity, surface area, and pore size, but is also primarily affected by surface functional groups that promote pseudocapacitive reactions [4,6,16,21]. This can be partly confirmed by the FTIR spectra of untreated biochar, which shows lower -OH intensities compared to treated biochar.

Table 2. Areal capacitance values of the Ti foil electrodes at different pyrolysis temperatures and treatment methods at scan rates of 5 mV/s.

Biochar (n = 4) (*n = 1)	Areal Capacitance at 5 mV/s (mF/cm2)	% RSD
Bare Ti Foil*	0.31	-
UB 700	55.30	25.72
UB 800	33.68	17.26
UB 900	20.70	26.74
PRTB 700	15.95	13.87
PRTB 800	11.14	28.22
PRTB 900	5.70	45.00
POTB 700	31.65	2.63
POTB 800	28.87	13.52
POTB 900	24.45	28.48

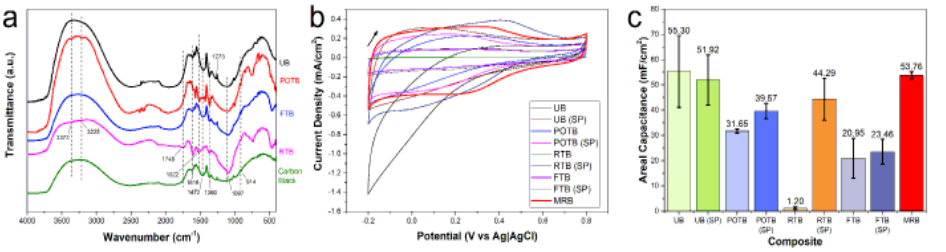

Figure 3. The (a) FTIR spectra of the treated biochars, (b) CV profiles of the treated biochar composites, and (c) bar graph of the areal capacitances of the composites derived from cyclic voltammetry.

Effect of chemical treatments. After treating crushed rice straw with HNO_3, the intensity of the -OH and C-O-C peaks increased, indicating enrichment of oxygen-containing groups, while the loss of the carbonyl C=O peak suggested lignin removal, as shown in Figure 2(a) [4,6]. Pyrolysis of pre-treated rice straw (PRTB) further increased the intensity of the -OH peak due to HNO_3 enrichment, which was even more pronounced in the spectra POTB. The peak around 1100 cm^{-1}, characteristic of ethers and pyranose ring groups, was preserved despite the extreme conditions of functionalization and pyrolysis [20]. This peak is sharper than in UB spectra, likely due to HNO_3's oxygen-enhancing effects (Figure 3(a)). These structures also help in biochar dispersion by providing binding sites for anionic surfactants like SDS and SDBS [4,17,22]. The RTB spectra show increased intensity at 1616 cm^{-1}, 1522 cm^{-1}, and 1366 cm^{-1} peaks, suggesting the formation of more aromatic and alkene structures. The sharper pyranose peak at 1097 cm^{-1} and the -OH peak at 3373 cm^{-1} indicate the addition and enrichment of oxygen functional groups on the biochar. However, the peak at 1748 cm^{-1} suggests the formation of -C=O functional groups, which can hinder the electroactive properties of RTB due to their poor electrochemical performance [5]. The FTB spectra also shows a sharper pyranose peak than the UB and POTB spectra, with little to no change in the -OH peak intensity at 3373 cm^{-1}. The increased intensity at 1616 cm^{-1} and 1472 cm^{-1} indicates the formation of aromatic groups.

Table 3. Areal capacitance values of the Ti foil electrodes at differently treated and spiked biochar at scan rates of 5 mV/s.

Biochar (n = 4)	Areal Capacitance at 5 mV/s (mF/cm2)	% RSD
UB	55.30	25.73
UB (SP)	51.92	19.05
POTB	31.65	2.63
POTB (SP)	39.57	7.76
RTB	1.20	51.50
RTB (SP)	44.29	18.79
FTB	20.95	37.82
FTB (SP)	23.46	20.95
MRB	53.76	2.62

After treatment and pyrolysis, the cyclic voltammograms of the biochar electrodes showed broad, leaf-like profiles, with peaks at 0.2 V and 0.4 V indicating faradaic or pseudocapacitive reactions (Figure 3(b)). The PRTB/Ti Foil electrodes showed much lower areal capacitance value of 15.95 mF/cm^2 than UB/Ti Foil electrodes with 55.30 mF/cm^2. This decrease is likely due to lignin degradation from HNO_3 treatment and pyrolysis, which may have resulted in the formation of less electrochemically active structures for capacitance [5], which are in contrast to similar works such as the study of Kim and colleagues [6]. Treatment of PRTB to POTB increased areal capacitance significantly to 31.65 mF/cm^2. This improvement suggests that HNO_3 treatment reintroduced redox-active O groups, enhancing redox potential and pseudocapacitive properties, as reflected in the larger redox peaks. The POTB/Ti Foil electrodes also displayed a more consistent leaf-shaped CV profile than UB/Ti Foil electrodes. The biochar RTB and FTB performed poorly compared to UB and POTB, especially RTB. The poor performance of RTB may be attributed to the formation of -C=O groups, which have poor electroactive performance [5]. While these electroactive functional groups may have burned off during the thermal flashing process of FTB, leading to lower areal capacitance [4,5,16].

Effect of physical treatments. After spiking of the biochar with carbon black, increases in the areal capacitance of the biochar were observed, particularly for RTB (SP), which is several orders of magnitude higher than RTB as shown in Figures 3(b) and 3(c). This shows that the addition of highly conducting material, such as carbon black, had promoted faster ion transport within the material. To improve the sorbent ability of biochar, its surface area should be maximized. [9]. A higher surface area and smaller pore diameters (Ø < 2 nm) should presumably lead to better electroactivity of the electrode composites. Wet milling with a planetary ball mill was used to grind the biochar with DI H_2O as the solvent media. The addition of solvent media has distinct advantages over dry milling as it improves particle dispersion while milling, reducing aggregation and leading to finer particles, as seen in the study of Peterson and colleagues [9]. Milling had a further beneficial effect on the preparation of biochar dispersion. The smaller MRB particles facilitated easier preparation, resulting in an ink-like viscosity and consistency, and its particles took longer to settle. Biochar is challenging to apply as an ink due to its poor dispersion in solvents [6], which was noted in all previous dispersions. The viscosity of conductive inks and dispersions helps stabilize them against precipitation and aggregation, which is essential to obtain reproductible results [23]. For the CV results, MRB with areal capacitance value of 53.76 mF/cm^2 (2.62 % RSD, n = 4) performed far better than POTB (SP) with 39.57 mF/cm^2 (7.76 % RSD, n = 4); closer to UB and UB (SP) in terms of values (Table 3). In addition, they had more consistent CV plots, which is also reflected in their % RSD, showing even permeation and flow within the material.

Table 4. Surface characteristics of rice straw biochar.

Sample	BET surface area (m^2/g)	BJH pore surface area (m^2/g)	BJH pore volume (cm^3/g)	BJH pore diameter (nm)
Carbon black	62.95	68.45	0.0986	2.66
UB	44.10	18.75	0.0142	1.43; 3.64
PRTB	171.22	78.35	0.0970	3.67
POTB	167.66	77.54	0.0916	3.74
MRB	224.85	193.50	0.2257	1.92

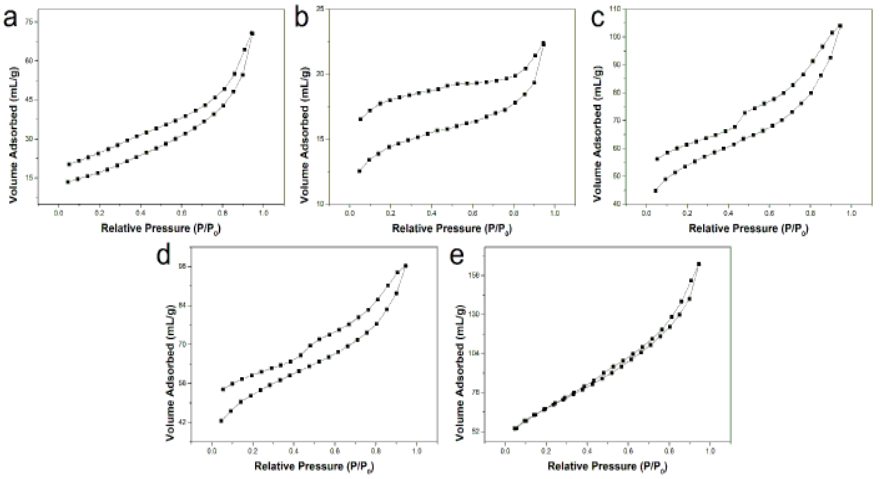

Figure 4. Physisorption isotherms of (a) carbon black, (b) UB, (c) PRTB, (d) POTB, and (e) MRB.

BET analysis. The biochar and carbon black physisorption isotherms show a Type IVa isotherm with an H4 hysteresis loop (Figure 4), indicating a mesoporous material with a complex pore structure and narrow neck [24,25]. The unclosed loop suggests pore or capillary condensation of N_2, or cavitation in larger pores during desorption [24,25]. This behavior is seen in activated carbons, and other materials like clays and zeolites [24]. Calculations using BJH theory confirm mesoporous diameters of the material (1 nm < Ø < 25 nm). Compared to carbon black, UB had a lower surface area due to its larger size, with an abundance of shallow micropores (Ø < 2 nm) in addition to mesopores. The increase in surface area and pore properties of PRTB show that the treatment of HNO_3 of the biomass before pyrolysis modified its structure at a microscale level [16]. However, post-treatment with HNO_3 reduced BET surface area from 171.22 m^2/g to 167.66 m^2/g, pore surface area from 78.35 m^2/g to 77.54 m^2/g, and volume from 0.0970 cm^3/g to 0.0916 cm^3/g. This decrease is similar to other literatures [5,26], probably from the binding of O_x-groups onto the pore surfaces and causing oxidation-induced structural collapse of the pores [5]. While PTRB had a higher surface area, it was also the one of the worst performing biochar for capacitance, showing that higher surface area doesn't directly correlate increased electroactivity [5]. Milling biochar doubled its surface area and helped expose smaller pores produced by the release of volatiles during pyrolysis [11,14], evidenced by the significantly higher pore surface area and smaller pore sizes of MRB. These properties contribute to the increased wettability of the material, allowing for the permeation of the electrolyte within biochar [16], leading to better electroactive performance and rate capability [7,27], and evidenced by its improved CV results. This shows that surface functionality, graphitization, and good porous structure contribute more towards a biochar's electrochemical properties [7,16].

Conclusion

Rice straw biochar was effectively prepared and analyzed for use in supercapacitor electrodes. Through cyclic voltammetry and BET analysis, the optimal method involved pyrolysis at 700 °C, combined with pre- and post-treatment using HNO_3, followed by adding 10 % (w/w) carbon black and wet milling. This process significantly increased particle size, surface area, and pore volume of MRB, contributing to its outstanding electrochemical performance attributed to its porous structure. Surface functional groups introduced during the treatment and milling procedures also improved electrode wettability, facilitating efficient ion transfer and storage. These results demonstrate substantial benefits of refining treatment methods to enhance the electrochemical capabilities of biochar. Furthermore, they show the potential to upcycle agricultural waste such as rice straw into valuable electroactive materials.

Acknowledgments

The authors would like to acknowledge the DOST Grants-in-Aid (GIA) Science for Change Program – Niche Centers in the Regions for R&D and the Philippine Council for Industry, Energy and Emerging Technology Research and Development for funding this project (DOST – NICER Project no. 8883). Sincere thanks to the Science Education Institute of the Department of Science and Technology (DOST – SEI) for the scholarship of one of the aurthors (DJGA).

Conflict of Interest

The authors declare that they have no known competing financial interests or personal relationships that could have appeared to influence the work reported in this paper.

Author Contributions

Conceptualization, David Joseph G. Alzate, Felicidad Christina R. Peñafiel, Christina A. Binag; Methodology, David Joseph G. Alzate, Felicidad Christina R. Peñafiel; Data collection, David Joseph G. Alzate; Analysis and interpretation of data, David Joseph G. Alzate, Felicidad Christina R. Peñafiel; Original draft preparation, David Joseph G. Alzate; Review and editing of the draft, Felicidad Christina R. Peñafiel, Christina A. Binag.

Institutional Review Board Statement

Not applicable.

Informed Consent Statement

Not applicable.

References

[1] Balingbing C, Van Hung N, Roxas AP, Aquino D, Barbacias MG, & Gummert M. An Assessment on the Technical and Economic Feasibility of Mechanized Rice Straw Collection in the Philippines. Sustainability 2020; 12(17), 7150. DOI: 10.3390/su12177150.

[2] Baptista JM, Sagu JS, KG UW, & Lobato K. State-of-the-art materials for high power and high energy supercapacitors: Performance metrics and obstacles for the transition from lab to industrial scale – A critical approach. Chemical Engineering Journal 2019; 374(April), 1153–1179. DOI: 10.1016/j.cej.2019.05.207.

[3] Ramirez FCR, Ramakrishnan P, Flores-Payag ZP, Shanmugam S, & Binag CA. Polyaniline and carbon nanotube coated pineapple-polyester blended fabric composites as electrodes for supercapacitors. Synthetic Metals 2017; 230(May), 65–72. DOI: 10.1016/j.synthmet.2017.05.005.

[4] Genovese M, Jiang J, Lian K, & Holm N. High capacitive performance of exfoliated biochar nanosheets from biomass waste corn cob. Journal of Materials Chemistry A 2015; 3(6), 2903–2913. DOI: 10.1039/c4ta06110a.

[5] Jiang J, Zhang L, Wang X, Holm N, Rajagopalan K, Chen F, & Ma S. Highly ordered macroporous woody biochar with ultra-high carbon content as supercapacitor electrodes. Electrochimica Acta 2013; 113, 481–489. DOI: 10.1016/j.electacta.2013.09.121.

[6] Kim HR, Lee JH, Lee SK, Chun Y, Park C, Jin JH, Lee HU, & Kim SW. Fabricating a modified biochar-based all-solid-state flexible microsupercapacitor using pen lithography. Journal of Cleaner Production 2021; 284. DOI: 10.1016/j.jclepro.2020.125449.

[7] Gomez-Martin A, Gutierrez-Pardo A, Martinez-Fernandez J, & Ramirez-Rico J. Binder-free supercapacitor electrodes: Optimization of monolithic graphitized carbons by reflux acid treatment. Fuel Processing Technology 2020; 199(November 2019), 106279. DOI: 10.1016/j.fuproc.2019.106279.

[8] Pourhosseini SEM, Norouzi O, & Naderi HR. Study of micro/macro ordered porous carbon with olive-shaped structure derived from Cladophora glomerata macroalgae as efficient working electrodes of supercapacitors. Biomass and Bioenergy 2017; 107(November), 287–298. DOI: 10.1016/j.biombioe.2017.10.025.

[9] Peterson SC, Jackson MA, Kim S, & Palmquist DE. Increasing biochar surface area: Optimization of ball milling parameters. Powder Technology 2012; 228, 115–120. DOI: 10.1016/j.powtec.2012.05.005.

[10] Lyu H, Yu Z, Gao B, He F, Huang J, Tang J, & Shen B. Ball-milled biochar for alternative carbon electrode. Environmental Science and Pollution Research 2019. DOI: 10.1007/s11356-019-04899-4.

[11] Lyu H, Gao B, He F, Zimmerman AR, Ding C, Huang H, & Tang J. Effects of ball milling on the physicochemical and sorptive properties of biochar: Experimental observations and governing mechanisms. Environmental Pollution 2018; 233, 54–63. DOI: 10.1016/j.envpol.2017.10.037.

[12] Ding Y, Wang T, Dong D, & Zhang Y. Using Biochar and Coal as the Electrode Material for Supercapacitor Applications. Frontiers in Energy Research 2020; 7(159). DOI: 10.3389/fenrg.2019.00159.

[13] Huang M, Dai B, Shi J, Li J, & Xia C. Sustainable Supercapacitor Electrode Based on Activated Biochar Derived from Preserved Wood Waste. Forests 2024; 15(1), 177. DOI: 10.3390/f15010177.

[14] Zhao B, O'Connor D, Zhang J, Peng T, Shen Z, Tsang DCW, & Hou D. Effect of pyrolysis temperature, heating rate, and residence time on rapeseed stem derived biochar. Journal of Cleaner Production 2018; 174, 977–987. DOI: 10.1016/j.jclepro.2017.11.013.

[15] Ehsani A & Parsimehr H. Electrochemical energy storage electrodes from fruit biochar. Advances in Colloid and Interface Science 2020; 284, 102263. DOI: 10.1016/j.cis.2020.102263.

[16] Dong K, Liu S, Guo F, Wang J, Tang B, Zhao N, Kong L, & Zhang Y. Facile synthesis of hierarchical porous carbon electrodes with 3D self-supporting structure and N/S self-doping for advanced energy storage device. Journal of Energy Storage 2023; 72(PA), 108218. DOI: 10.1016/j.est.2023.108218.

[17] Jin H, Wang X, Gu Z, & Polin J. Carbon materials from high ash biochar for supercapacitor and improvement of capacitance with HNO3 surface oxidation. Journal of Power Sources 2013; 236, 285–292. DOI: 10.1016/j.jpowsour.2013.02.088.

[18] Malik K, Sharma A, Harikarthik D, Rani V, Arya N, Malik A, Rani S, Sangwan P, & Bhatia T. Deciphering the biochemical and functional characterization of rice straw cultivars for industrial applications. Heliyon 2023; 9(6), e16339. DOI: 10.1016/j.heliyon.2023.e16339.

[19] Khedulkar AP, Pandit B, Dang VD, & Doong R an. Agricultural waste to real worth biochar as a sustainable material for supercapacitor. Science of the Total Environment 2023; 869(December 2022), 161441. DOI: 10.1016/j.scitotenv.2023.161441.

[20] Wu W, Yang M, Feng Q, McGrouther K, Wang H, Lu H, & Chen Y. Chemical characterization of rice straw-derived biochar for soil amendment. Biomass and Bioenergy 2012; 47, 268–276. DOI: 10.1016/j.biombioe.2012.09.034.

[21] Rahman MZ, Edvinsson T, & Kwong P. Biochar for electrochemical applications. Current Opinion in Green and Sustainable Chemistry 2020; 23, 25–30. DOI: 10.1016/j.cogsc.2020.04.007.

[22] Islam R, Khair N, Ahmed DM, & Shahariar H. Fabrication of low cost and scalable carbon-based conductive ink for E-textile applications. Materials Today Communications 2019; 19(December 2018), 32–38. DOI: 10.1016/j.mtcomm.2018.12.009.

[23] Htwe YZN, Chow WS, Suriati G, Thant AA, & Mariatti M. Properties enhancement of graphene and chemical reduction silver nanoparticles conductive inks printed on polyvinyl alcohol (PVA) substrate. Synthetic Metals 2019; 256(August), 116120. DOI: 10.1016/j.synthmet.2019.116120.

[24] Thommes M, Kaneko K, Neimark A V., Olivier JP, Rodriguez-Reinoso F, Rouquerol J, & Sing KSW. Physisorption of gases, with special reference to the evaluation of surface area and pore size distribution (IUPAC Technical Report). Pure and Applied Chemistry 2015; 87(9–10), 1051–1069. DOI: 10.1515/pac-2014-1117.

[25] Tsai W-T, Hsu C-H, & Lin Y-Q. Highly Porous and Nutrients-Rich Biochar Derived from Dairy Cattle Manure and Its Potential for Removal of Cationic Compound from Water. Agriculture 2019; 9(6), 114. DOI: 10.3390/agriculture9060114.

[26] Liu MC, Kong L Bin, Zhang P, Luo YC, & Kang L. Porous wood carbon monolith for high-performance supercapacitors. Electrochimica Acta 2012; 60, 443–448. DOI: 10.1016/j.electacta.2011.11.100.

[27] Sun C, Li X, Cai Z, & Ge F. Carbonized cotton fabric in-situ electrodeposition polypyrrole as high-performance flexible electrode for wearable supercapacitor. Electrochimica Acta 2019; 296, 617–626. DOI: 10.1016/j.electacta.2018.11.045.